Digestive Diseases and Sciences, Vol. 43, No. 4 (April 1998), pp. 683–693

Biomagnetic 3-Dimensional Spatial and Temporal Characterization of Electrical Activity of Human Stomach

H.D. ALLESCHER, MD, PhD, K. ABRAHAM-FUCHS, PhD, R.E. DUNKEL, Dipl.-Phys, and M. CLASSEN, MD, PhD

Biomagnetic measurements are based on the noninvasive recording of magnetic signals produced by biological sources such as nervous system and muscle. The aim of this study was to obtain multichannel magnetic field recordings from the human gastrointestinal tract and to localize the sources of these signals three-dimensionally. The magnetic field was recorded in eight human healthy subjects using a sensor array with 37 superconducting quantum interference devices (SQUIDs); an electrogastrogram was recorded simultanously. Biomagnetic source localization was carried out with an iterative nonlinear optimization algorithm using the model of an equivalent current dipole (ECD) and correlated to magnetic resonance imaging (MRI) in four volunteers. Magnetogastrograms and electrogastrograms demonstrated a similar frequency distribution with a peak at 3/min. In all subjects the centers of the calculated dipoles plotted vs time showed a characteristic migration across the stomach area. One volunteer demonstrated tachygastric episodes, during which his magnetic field amplitudes increased fivefold and his dipole migration disappeared. In absence of an attack his recordings changed to normal. This demonstrates multichannel magnetic recordings can be used to localize the sources of the biomagnetic field, which could be useful for the understanding of motility disturbances.

KEY WORDS: biomagnetism; slow-wave activity; tachygastria.

Magnetic fields are created by moving charges, ie, by currents and changing electric fields. In principle the electric or magnetic fields can be measured. Measuring the electrical field is well established, but only extracellular currents can be measured and the differences in the electric conductivity of tissues cause distortion of the field (1–10). On the other hand, magnetic fields are less disturbed by the differences in the electric conductivity of tissues; even the high resistance of the cell membrane does not change the field. By this means, a recording of intracellular currents is also possible. The main disadvantages of the recording of magnetic fields are the high demands on the recording equipment, because the fields generated in the body are some million times weaker than the magnetic field of the earth. Thus the measurements have to be carried out in a magnetically shielded room and a superconducting quantum interference device (SQUID) has to be used for recording. Additionally for field location, multichannel recordings are required. As the signal amplitude compared to the environmental noise is low, summation of a recurrent cycling signal is often helpful to improve the

Manuscript received May 31, 1997; revised manuscript received December 15, 1997; accepted December 29, 1997.

From the II. Medizinische Klinik und Poliklinik der TU München, Ismaningerstr. 22, 81675 München; and Siemens AG Medical Engineering Group, Henkestrasse, 91054 Erlangen, Germany.

Address for reprint requests: Priv.- Doz. Dr. med. Hans-Dieter Allescher, II. Medizinische Klinik und Poliklinik der TU München, Ismaningerstr. 22, 81675 München, Germany.

signal-to-noise ratio. Based on this technique it is possible to calculate a theoretical electrical current dipole, representing the generator of the magnetic field as has been shown for the brain (1–5) and the heart (6–10).

The smooth muscle layer of the gastrointestinal tract is characterized by a periodic cyclic electrical activity that can be detected by mucosal, serosal, or surface electrodes. This electrical activity shows specific and characteristic frequencies in the various regions of the gastrointestinal tract (11–20). This cyclic electrical activity, which has been named electrical control activity or slow waves, is due to a nerve-independent mechanism that causes a depolarization of the cell membrane. Recent studies have suggested that they might be generated by interstitial cells of Cajal located at the border of the muscularis propria and the subserosa (21).

Biomagnetic measurement devices have been previously used in the gastrointestinal tract in two different ways. The first application was the detection of ferromagnetic pellets that were swallowed by the patient in order to be localized and thus estimate gastric motility and emptying. Even though this method can not strictly be regarded as biomagnetic recording, biomagnetic measurement devices were used to determine and calculate the position of the pellets. Such a three-dimensional path of the pellets through the gastrointestinal tract can be monitored across time (22–28). The electrophysiological gastric activity itself had been measured using single- and four-channel SQUIDs in New Zealand rabbits and recently in humans (29–32). In all studies a strong correlation between the electric and magnetic signal had been seen, thus demonstrating the fact that the basic electric rhythm can be measured magnetically. In the animal studies the basic electrical rhythm frequency decreased significantly after artificial mesenteric ischemia (29, 30). This provided the opportunity to detect intestinal ischemia noninvasively. A three-dimensional source localization was not possible from these measurements, since for the source localization a multichannel system with at least 15 to 20 sensors is necessary (33).

The aim of the present study was to apply the technique of multichannel biomagnetic recording of electrical activity to the gastrointestinal tract and especially to the stomach. By using multichannel biomagnetic recordings, our aim was to characterize the spatial and temporal distribution of the magnetic fields of the stomach and, using an adequate model, to estimate the three-dimensional distribution of electrical activity of the stomach in normal human volunteers.

MATERIALS AND METHODS

Subjects. All eight volunteers were healthy males, ranging in age from 20 to 40 years. When choosen for the study they showed no gastroenterologic symptoms and had no history of a major gastrointestinal disease. All subjects underwent recordings fasted and fed, two underwent an additional session with the administration of cisapride. For the fasted condition, the volunteers were studied after an overnight fast (minimum 8 hr). The fed condition was measured after a standardized breakfast consisting of 200 ml orange juice, 1 cup of coffee, 2 rolls filled with sausage (total calorie content: 2500 kJ). Cisapride was applied perorally in a dose of 10 mg as suspension 15 min before the next recording.

By chance one volunteer demonstrated a tachygastric attack during two recording sessions. During these attacks he reported mild dyspeptic symptoms. This volunteer was excluded from the normal study subjects, but his recording and evaluation are added separately.

Magnetic Recording. The magnetic field recordings were carried out in eight healthy males with the multichannel biomagnetic recording system Krenikon (34, 35). The Krenikon consists of a liquid-helium-cooled sensor array, enclosed in a fiberglass cryostat, located in a magnetically shielded room. The sensor array consists of 37 DC SQUIDs coupled to an array of axial first-order gradiometers, with a baseline of 7 cm. The pickup coils of 2.7 cm diameter are densely packed over a flat total circular area of 19 cm diameter. Since the measurements reported here were carried out in a laboratory setup, typically only 32 of the 37 magnetic channels were used.

The sensor module was oriented such that the center of the magnetic recording area was in the medial line and at the height of lower border of the chest. The recording system was moved up to 2 cm above the abdominal wall to allow free breathing without direct contact to the sensor.

Electrical Recording. The cutaneous electrogastrogram was recorded simultaneously in all subjects by four cutaneous electrodes located in the epigastrium. Additionally the respiration was monitored by a nonmagnetic respiratory belt.

Data Acquisition and Processing. After on-line antialiasing filtering (Bessel filter, linear phase, attenuation 48 dB/octave with a cutoff frequency selectable in a wide range) of the magnetic field data of the 32 channels the data were digitized using a 12-bit AD converter with a sampling frequency of 40 Hz and stored on a hard disk. The magnetic and electrical signals were subjected to a digital bandpass filter (low-pass filter: −3 dB at 0.12 Hz and −30 dB at 0.18 Hz, and high-pass filter: cutoff frequency 0.12 Hz). The electrogastrogramm was treated in the same way. These frequencies were chosen to eliminate artifacts produced by respiration and the heart activity.

Pattern Recognition and Summation Signal. In order to further analyze magnetogastrogram (MGG) data, noise reduction is essential. If the signal represents repetitive events, it is common to search for similar events. The

rationale of this method is the assumption that single unexpected events result from artifacts (eg, used for calculation of evoked potentials in the brain). If the signal represents repetitive events recorded from different leads, which means different directions, it is then possible to search for similar events over time and over the spatial distribution in all recording sites. Since gastric activity is a periodic process, an automated event detection algorithm, originally developed for the detection of epileptic spike-wave events in the magnetoencephalogram, was used for this purpose (36). The algorithm assumes that an event is completely characterized by the temporal wave form in each sensor and the spatial field pattern at each acquisition point during the event. Thus the whole spatiotemporal multichannel data matrix of an interactively selected template wave cycle is taken, and the temporal cross-correlation of the template signal with the whole data set is calculated. Maxima in this cross-correlation function indicate the time-aligned occurrence of sufficient similar gastric cycles, which are then averaged. Similar patterns detected were time-aligned and averaged. Possible artifacts were studied by dummy recordings where no subject was in the recording chamber. The further technical details of this pattern recognition algorithm are given elsewhere (36).

Three-Dimensional Localization. Three-dimensional source localization was carried out at 0.1-sec intervals over the whole wave cycle. First, the measured magnetic field distribution of the 32 different magnetic sensors was visualized on an a two- or three-dimensional grid (isocontour field maps). The isocontour field maps contain the whole information about the underlying physiological process, but it is common to reduce the information to calculated sources of the field distribution. For that, a model is needed, because arithmetically every field map has a unlimited number of possible sources generating the field. The model limits the arithmetically possible sources to physiologically acceptable sources. The most easy, striking, and so far in practice the only model used in medicine is the model that calculates a dipole as the source of the isocontour field maps [eg, the vector (dipole) in the vector ECG]. Thus for three-dimensional source localization of the electrical activity of the stomach, the model of an equivalent current dipole (ECD) immersed in the homogeneous half space was used. The boundary surface of the half space represents the frontal wall of the body. It is known that the ECD is not in all cases the ideal source model since an ECD only describes activity confined to a small tissue volume, ie, on the order of 10 cubic centimeters, but it was supposed to be adequate as an approach in this comparative study. More complex source models, such as distributed current reconstruction by means of the minimum norm method, which are further steps in future, are limited by the power of current computer systems.

After having localized dipoles at selected time points in the data set, several plausibility criteria are applied to the solutions to check for the reliability of each dipole (37). The most important validation criterion is the goodness of fit, which quantifies how well the dipole solution explains the measured field map. The goodness of fit is usually given as fraction of the total measured field energy that is explained by the dipole, typically in the range of 0.90 to 0.99. In our evaluations we have chosen a threshold of 0.96 for acceptance of a dipole solution. Other criteria that may be used for dipole validation if there is prior knowledge available from electrophysiology are nerve conductance velocity or slow-wave conductance velocity, which is related to the distance between successive dipole positions, and action potential duration or slow-wave duration, which is related to the spatial stability of a dipole location. Neither criterion has been applied in the evaluation of the results presented in this paper, but may help in further interpretation of these phenomena in the future.

Image Fusion of MGG and MRI. In order to allow the visualization of the three-dimensional MGG source localization in relation to the patient's anatomy, MR images were obtained from four volunteers. Four external markers connected to a cross-shaped plastic frame were taped to the subject's chest in order to allow a transformation from the biomagnetic coordinate system to MRI coordinates. The markers contained small current loops during the MGG measurements, which can be localized from the biomagnetic measurement system, and were replaced by a contrast agent (silicone jelly) during the MR measurements. By use of the four individual points, the coordinate transformation matrix is calculated, and the dipole locations are directly projected into the respective MR slice. The dipole position at each evaluated time point is visualized in the MR image by small red markers (crosses).

RESULTS

Field Amplitude. When recording from the stomach area, a typical wave pattern could be detected in all magnetic channels that resembled the simultaneously recorded electrical activity of the electrogastrogram. On average, 30 ± 14 similar wave cycles were detected during the 20-min recording period by the pattern recognition algorithm, and they were further used for summation of the signal. Thus the pattern recognition algorithm detected half the expected wave cycles using 3 cycles/min as working hypothesis. The undetected wave cycles result from artifacts, such as movement of the volunteer, which

TABLE 1. DURATION AND AMPLITUDE OF MAGNETOGASTRIC RECORDINGS

	N	*Duration of averaged wave cycle (sec, mean ± SD)*	*Amplitude (pT)*	
			Maximum	*Minimum*
Total	17	21.8 ± 3.4	2.6 ± 1.2	−2.3 ± 0.9
Fasted	6	21.9 ± 3.3	1.92 ± 0.8	−1.85 ± 0.68
Fed	9	21.5 ± 3.8	3.33 ± 1.1*	−3.06 ± 1.02*
Cisapride	2	25.7 ± 1.8	1.64 ± 0.7	−2.4 ± 0.5
Tachygastria	†	11.4 ± 0.3	12.5 ± 2.3	−14.5 ± 2.2

* Significantly different compared to fasted ($P < 0.05$).

† The values were obtained in the same patient in two different recording sessions.

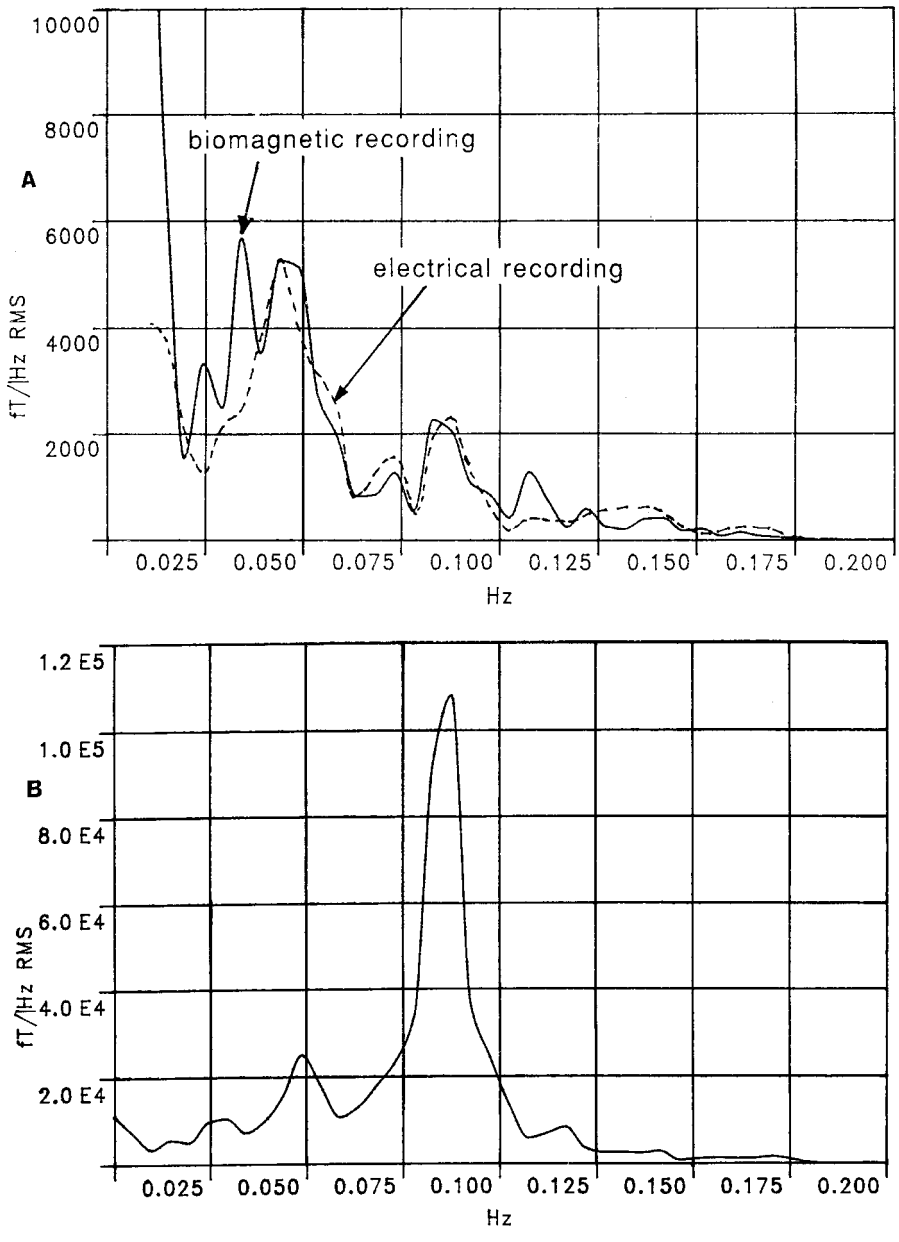

Fig 1. Frequency spectrum of the electrical and the magnetic recording in a normal volunteer (A) and in a volunteer with tachygastria (B). (A) The electrical recording is also plotted and the bandpass filter is switched off, showing the close reationship with the biomagnetic recording and the artifacts produced by respiration and heart activity. In the normal volunteer a biomagnetic dominant frequency of 0.035 and 0.045 Hz was observed according to the normal gastric activity. In the volunteer with tachygastria, a biomagnetic dominant frequency of 0.085 Hz occurred. (fT/Hz RMS = femtotesla per hertz root mean square.)

could not be completely avoided during the recording periods.

The magnetic field recordings typically showed amplitudes in the range of 0.5–4 pT during the maximum of these cycles. The magnetic field strength of the recordings in all fasted volunteers was smaller than after ingestion of food (Table 1). Yet these amplitude values can only be taken as a qualitative indication, since the amplitude depends on both electrical stomach activity and distance of the SQUID sensors to the muscle. This depends on placement of the SQUID multichannel array and the physical constitution of

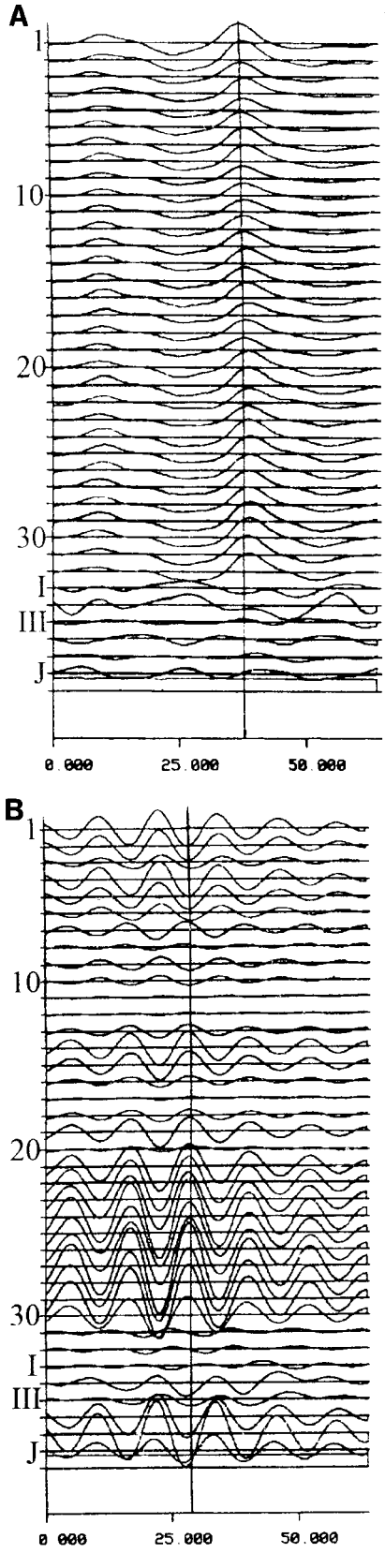

the volunteer. The quantitative comparison of fasted and fed state is correct, since the same volunteers with the same sensor positions are examined in fasted and fed state.

Frequency Spectrum. When the frequency spectrum of the magnetic signal was determined by fast Fourier analysis and compared to the frequency spectrum of the electrical signal, a close relationship between the two signals could be observed (Figure 1A).

In one volunteer an atypical high frequency of the electrical and magnetic waves was observed. On the basis of the electrogastrogram this volunteer was diagnosed as having a tachygastric episode and was excluded from normal volunteers and treated separately (Figure 1B). At the time of the tachygastria, the volunteer had only mild dyspepsia but no other abdominal symptoms. The tachygastria was demonstrated on two occasions during two different recording sessions after a pause of about 30 min. In one recording session the tachygastria ceased after 20 min and electrical signals of normal amplitude and frequency were recorded.

Averaged Wave Cycles. The averaging of the detected events resulted in a sinusoidal summation wave with a mean duration of the positive half of the wave cycle of 10.6 $\pm$ 1.7 sec and of the negative half of the wave cycle of 11.2 $\pm$ 2.2 sec and a total wave duration of 21.8 $\pm$ 3.4 sec (Figure 2A). From this wave duration, a mean frequency of 2.8 $\pm$ 0.4 cycles/min was calculated.

The mean maximum amplitude of the averaged magnetic waves of all recordings was 2.65 $\pm$ 1.18 pT, and the mean minimum amplitude was -2.28 ± 0.87 pT. The values for mean duration and minimum and maximum amplitude for the different subgroups [fasted state ($N = 8$), fasted state plus cisapride ($N = 2$), and fed state ($N = 8$)] as well as for the patient with tachygastria are given in Table 1.

No significant difference in the mean duration of the averaged wave of the magnetic signal in the fasted and fed state was observed. However, the amplitude of the magnetic wave signal was significantly enhanced after ingestion of a continental breakfast.

The averaged wave from the volunteer who had

Fig 2. Averaged wave cycles of the magnetic signal in a normal volunteer (A) and in a volunteers with tachygastria (B). The averaged wave cycles are calculated as the summation of all wave cycles detected by the pattern recognition algorithm during a recording session. The figure shows the averaged cycles for the 32 recording channels of the magnetogastrogramm (1–32) and recording channels I, II, III, O, A, and J of the electrogastrogram (I–III–J). The abscissa is scaled in seconds.

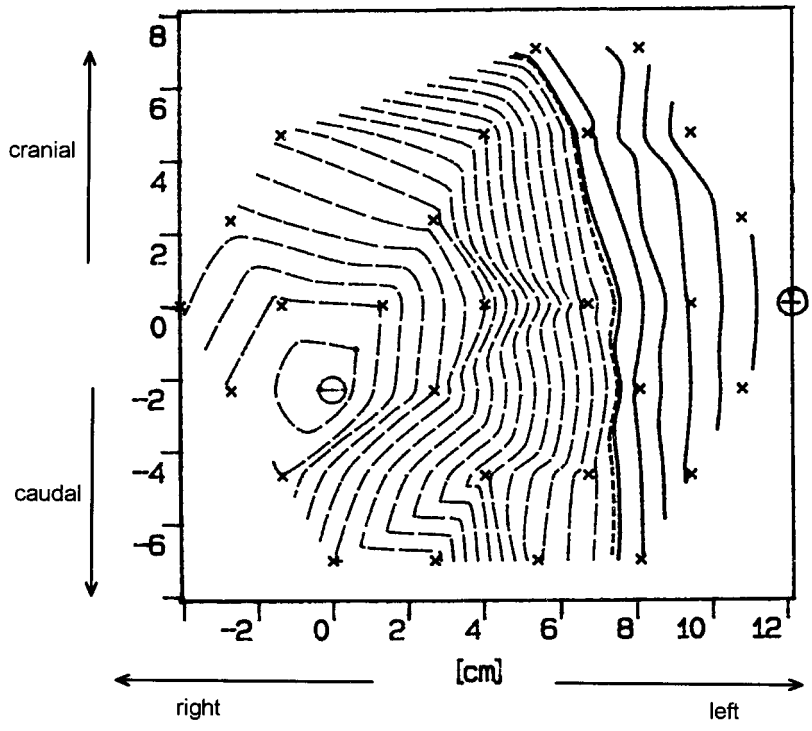

Fig 3. Example of a magnetic field distribution. Similar magnetic field distributions were calculated every 100 msec for the whole wave cycle. The dipoles are then calculated from this field distributions.

tachygastria in the electrical and in the biomagnetic signal is shown in Figure 2B. If we assume a normal range of the parameters with means of ±2 SD, the duration of the average signal as well as the amplitude of the magnetic waves were far outside this normal range. The amplitude of the magnetic signal was five times higher than the average amplitude in the other volunteers and the duration of the magnetic waves was only half that of the other volunteers, corresponding to an average frequency of 5.3/min. After the tachygastria had ended and the frequency of the gastric activity was in the normal range again, magnetic amplitude and duration of the half cycles were in the same range as in other volunteers.

Magnetic Field Distribution (Field Map). The averaged wave cycles can also be displayed in form of the spatial magnetic field distribution across all magnetic channels (isocontour field maps). An example of magnetic field maps is given in Figure 3. This field maps show the magnetic field distribution above the right abdominal region. The magnetic field lines connect areas of identical magnetic field strength.

Dipole Propagation. The dipole propagation of the normal volunteers (fasted and fed) and the tachygastric volunteer in absence of an epigastric attack shows a characteristic migration of the ECD during the wave cycle (Figure 4A, Table 2). This migration is distinctly reduced in the tachygastric attacks (Figure 4B, Table 2).

Fusion of Three-Dimensional Distribution of ECDs with MR Image. Having established a common reference system for MGG and MR measurements as described above, the schematic representation of the dipole distribution can also be projected directly into the corresponding MR image of this subject in order to correlate the three-dimensional distribution of the ECD localization with anatomical structures. In all four volunteers (normal), who underwent MRI examination, the three-dimensional ECD localization is closely correlated with the stomach area. An example is given in Figure 5.

DISCUSSION

The present study demonstrates that biomagnetic recording of electrical activity of the human stomach can be performed with a multichannel recording system. With such a multichannel system, which is already used clinically in neurology and cardiology, a three-dimensional localization of the equivalent di-

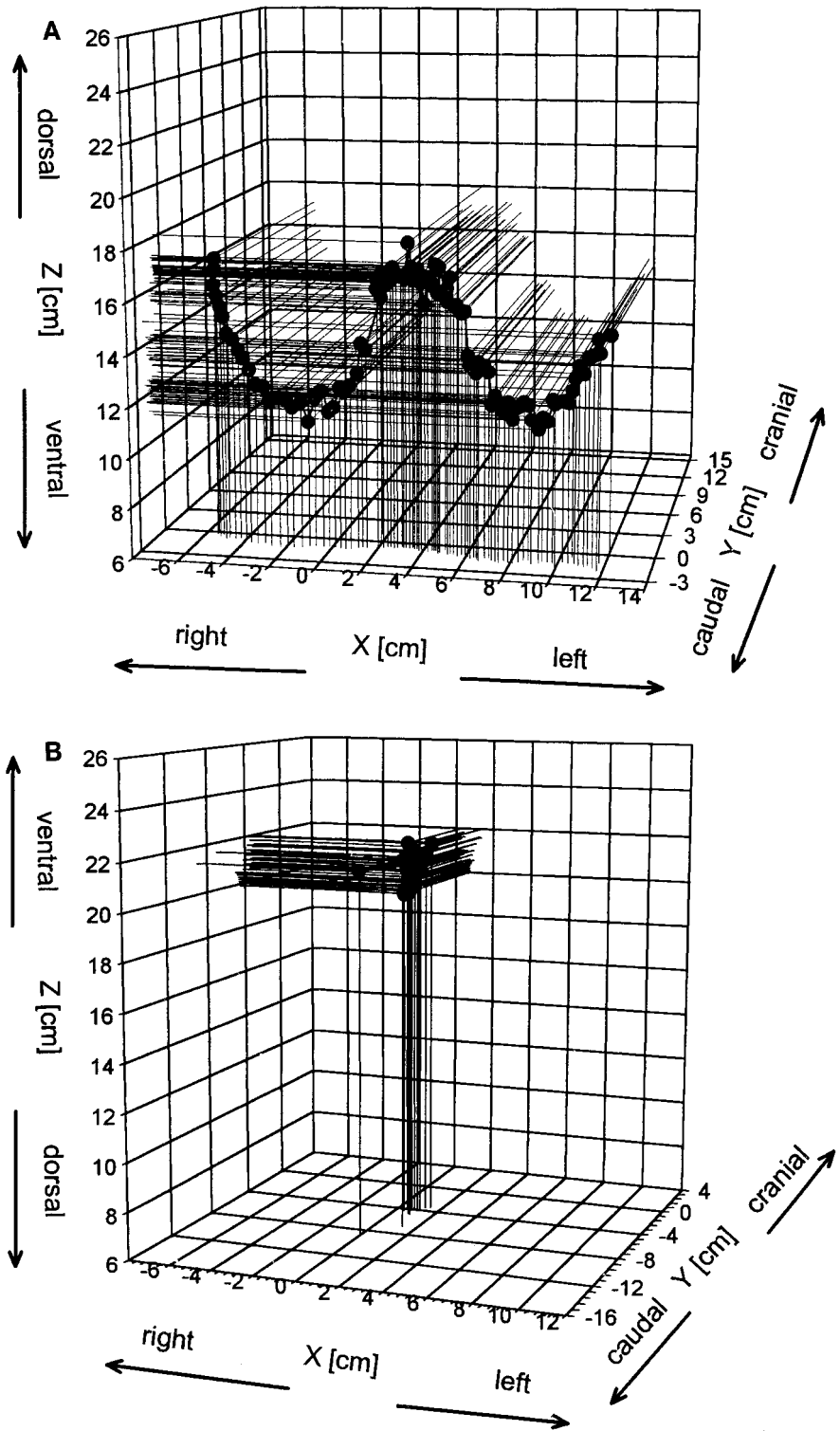

Fig 4. Three-dimensional dipole propagation of the volunteer with tachygastria without a tachygastric attack (A) and during an attack (B). The dipole propagation of the volunteer with tachygastria is distinctly reduced. The *x* axis points from right to left (zero at the medial line), the *y* axis from feet to the head (zero at the costal arc), and the *z* axis from back to front (zero at bed level).

TABLE 2. VOLUME OF MINIMAL CUBOID CONTAINING ALL DIPOLE CENTERS DURING A RECORDING SESSION

	Recording session											
										Tachygastric volunteer		
	Normal volunteers									*Without*	*During attack*	
	1	*2*	*3*	*4*	*5*	*6*	*7*	*8*	*9*	*10*	*11*	*12*
Volume (cm^3)*	1100	440	1,500	2,700	900	16,000	7,500	1,200	11,700	5,500	190	25

*Calculated as the product of the difference between the smallest and the largest value for the *x*, *y*, and *z* direction.

poles, representing the electric activity, can be performed. Biomagnetic signals have their origin in electric currents that occur sporadically or periodically. Such currents generate electric and magnetic fields according to the law of electrodynamics. A major advantage of the magnetic field is that magnetic field lines are less influenced by the surrounding body tissue. In contrast, electrical field lines are changed quite substantially due to conduction inhomogeneity of the various body tissues. Therefore the electrical fields that can be detected on the body surface are inhomogeneous and deformed, which makes a three-dimensional localization imprecise or impossible. For this reason the three-dimensional localization using magnetic fields is much more precise and reliable (3). An additional advantage is that the magnetic fields can be recorded outside the organism, even without making any body contact. A major disadvantage is that the biomagnetic fields are usually very weak, in general 10^6 times smaller than the magnetic field of the earth. In order to detect biomagnetic fields generated by biological current sources, highly sensitive detectors such SQUIDs and a magnetically shielded room are needed (35).

The current study describes the three-dimensional distribution of the current sources of the human stomach in normal healthy volunteers for the first time. Despite the fact that this three-dimensional current localization shows interindividual variations, several typical patterns could be observed. We demonstrated that with use of a pattern recognition algorithm the magnetic activity can be detected and the individual waves can be used for wave summation to improve the signal-to-noise ratio. The summation of the wave signal finally leads to a rather homogenous magnetic field (isocontour field maps), which can be used for dipole location. The calculated dipoles are arranged in or closely around the stomach region. In this respect, the activity is similar to the vector magnetocardiogram.

By chance one volunteer had a tachygastric attack during two different recording sessions. During his attacks he showed a higher frequency and a higher field amplitude. Additionally the dipole migration disappeared. This finding might be helpful for the localization of pacemakers of tachygastric activity.

When trying to correlate the current dipole localization with physiological electrical phenomena, several factors have to be kept in mind. First the signal baseline, which is important for ECD localization, can not be determined as easily as in the heart. In the heart an electrically quiet period can be assumed in the T-P interval. This assumption is not possible in the stomach, as there is at least one slow wave migrating from the proximal to the distal stomach. A shift of the baseline on the other side would cause a systematic shift of the three-dimensional ECD localization.

A second limitation is the model of the equivalent current dipole used for the three-dimensional localization. This model proves to be true only for a single current dipole generating the magnetic field. As the slow waves are not spatially homogeneous but spread around the circumference of the stomach, only a summation "vector" signal can be localized. Additionally there is evidence that while one slow wave is still present in the terminal antrum, the next slow wave will already be generated in the pacemaker region. Therefore the status of the presence of two slow waves on the stomach will occur. Therefore it is surprising to obtain a rather homogeneous 3-D localization, but it has to be kept in mind that this only reflects the localization of the summation vector.

To date in gastroenterology the use of SQUIDs is limited on basic research. The electrophysiological gastric activity itself had been measured using single-

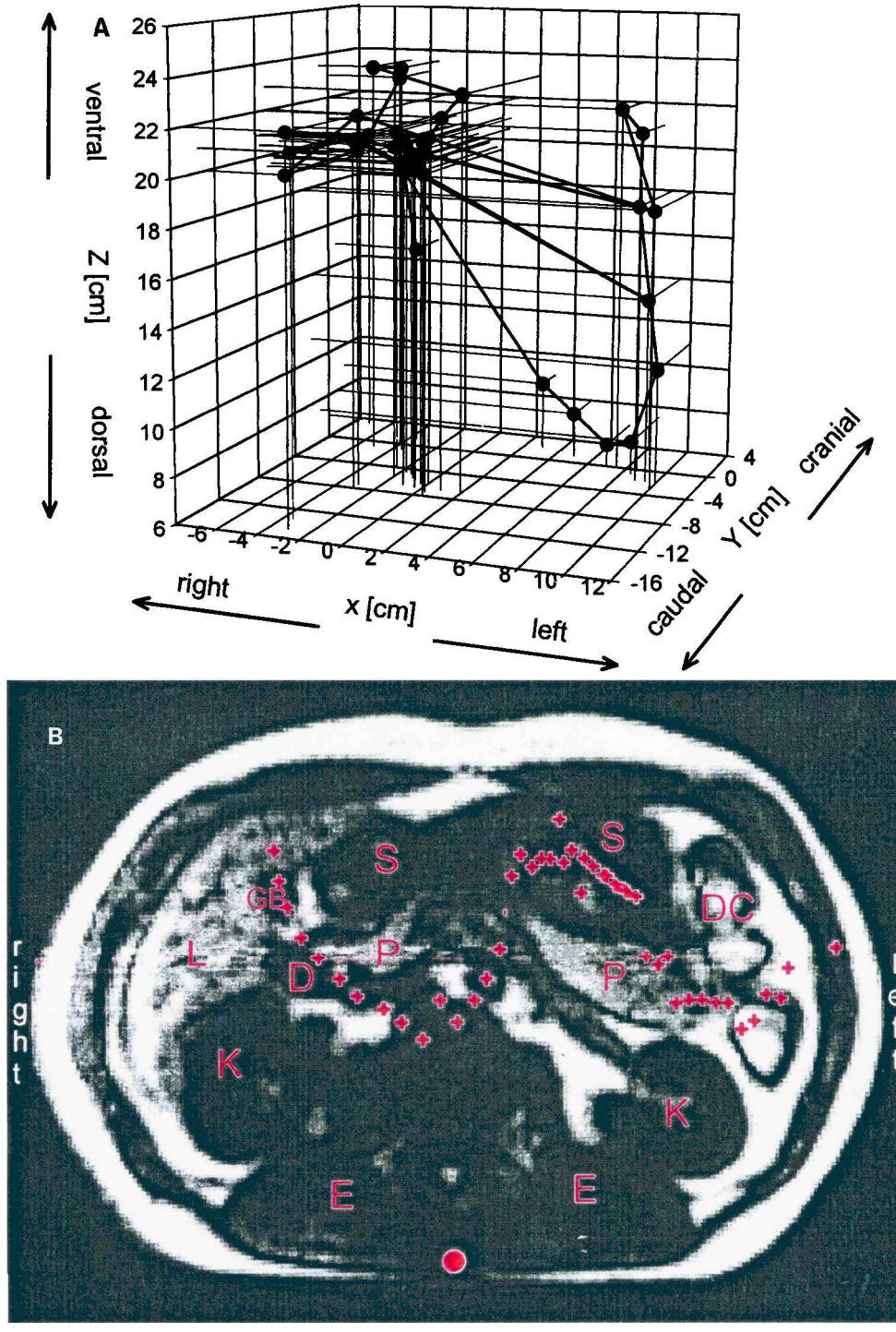

Fig 5. Three-dimensional dipole propagation (A) of a volunteer who underwent MR imaging and fusion with MR image in *x–z* (transverse) slize (B). The *x* axis points from right to left (zero at the medial line), the *y* axis from feet to the head (zero at the costal arc), and the *z* axis from back to front (zero at bed level). The red point marks zero in the MRI. A dipole center is calculated every 100 msec. For better clarity only every second dipole is plotted in the MR image. The dipoles form a transverse path across the stomach for about 10 sec in a sinusoidal shaped wave in the horizontal axis (shown), whereas before and after this characteristic distribution more localized dipoles were found in the proximal (corpus) and the distal (antrum) stomach (not shown). L: liver; GB: gallbladder; K: kidney; E: erector trunci muscle; P: pancreas; D: duodenum; S: stomach; DC: decending colon.

and four-channel SQUIDs in New Zealand rabbits and recently in humans (29–32). Animal studies provided the opportunity to detect intestinal noninvasive ischemia with this technique (29, 30). Our study provided the chance to detect and localize abnormalities in gastric electric activity. Until now, no clinical validation had been undertaken to show that these effects have clinical value. However, the improved spatial and temporal resolution suggests a possible diagnostic advantage to other methods such as the electrogastrogram. Nevertheless, the cost of the apparatus will be a major disadvantage. Further research on the SQUID technique will improve its performance and reduce the cost, and advances in computer technology will allow more power in dipole calculation. A better algorithm will allow working with a worse signal-to-noise ratio, thus measurements in a more noisy environment become possible and cost-intensive shielding of the examination room might be reduced. Additional more realistic models dealing with multiple dipoles are possible. In Russian hospitals SQUIDs are installed in unshielded rooms and have been used to detect the basic electrical rhythm (38). As biomagnetic multichannel devices will become available for clinical use in neurology and cardiology (by 1997 a total of 16 devices will be installed in Germany for clinical research), this technology will be available in an increasing number of clinics, which might also make possible clinical trials in gastroenterology.

ACKNOWLEDGMENTS

We acknowledge the expert support and help during the experiments of P. Wegener and R. Killmann, Siemens AG Medical Engineering Group.

REFERENCES

1. Barth DS, Sutherling WW, Engle J Jr, Beatty J: Neuromagnetic evidence of spatially distributed sources underlying epileptiform spikes in the human brain. Science 223:293–296, 1984
2. Sutherling WW, Crandall PH, Engel J Jr, Darcey TM, Cahan LD, Barth DS: The magnetic field of complex partial seizures agrees with intracranial localizations. Ann Neurol 21:548–558, 1987
3. Vieth J: Biomagnetische Vielkanaluntersuchungen am Gehirn. Dtsch Ärzteblatt 89:B283–B286, 1992
4. Cheyne D, Weinberg H, Gaetz W, Jantzen KJ: Motor cortex activity and predicting side of movement: Neural network and dipole analysis of pre-movement magnetic fields. Neurosci Lett 188:81–84, 1995
5. Stefan H, Schueler P, Abraham-Fuchs K, Schneider S, Gebhardt M, Neubauer U, Hummel C, Huk HJ, Tierauf P: Magnetic source localization and morphological changes in temporal lobe epilepsy: Comparison of MEG/EEG, ECoG and volumetric MRI in presurgical evaluation of operated patients. Acta Neurol Scand Suppl 152:83–88, 1994
6. Fenici RR, Masselli W: Magnetocardiography: Perspectives in clinical application. IEEE, Proceedings, 8th Annual Conference Society Engineering in Medicine and Biology 1986, 439 pp.
7. Moshage W, Achenbach S, Weikl A, Gohl K, Bachmann K, Abraham-Fuchs K, Harer W, Schneider S: Clinical magnetocardiography: experience with a biomagnetic multichannel system. Int J Card Imaging 7:217–223, 1991
8. Weismuller P, Abraham-Fuchs K, Schneider S, Richter P, Kochs M, Edrich J, Hombach V: Biomagnetic noninvasive localization of accessory pathways in wolff-parkinson-white syndrome. Pacing Clin Electrophysiol 14:1961–1965, 1991
9. Moshage W, Achenbach S, Gohl K, Weikl A, Bachmann K, Wegener P, Schneider S, Harer W: Biomagnetic localization of ventricular arrhythmias. Radiology 180:685–692, 1991
10. Nenonen J, Purcell CJ, Horacek BM, Stroink G, Katila T: Magnetocardiographic functional localization using a current dipole in a realistic torso. IEEE Trans Biomed Eng 38:658–664, 1991
11. Bass P: Electric activity of smooth muscle of the gastrointestinal tract. Gastroenterology 49:391–394, 1965
12. Becker JM, Duff WM, Moody FG: Myoelectric control of gastrointestinal and biliary motility: A review. Surgery 89:466–477, 1981
13. Laplace JP: Motricité de l'intestin grele: Organisation, regulation et fonctions. Quinze ans de recherches sur les complexes migrants. Reprod Nutr Dev 24:707–765, 1984
14. Sarna SK: Cyclic motor activity; migrating motor complex: 1985. Gastroenterology 89:894–913, 1985
15. Karaus M, Wienbeck M: Dickdarmmotilitat. Fortschr Med 107:356–360, 1989
16. Bazzocchi G, Lanfranchi GA: Metodi di analisi dell'attivita motoria gastrointestinale. Minerva Chir 46(suppl):19–25, 1991
17. Chen J, McCallum RW: Electrogastrography: measurement, analysis and prospective applications. Med Biol Eng Comput 29:339–350, 1991
18. Sarna SK: Colonic motor activity. Surg Clin North Am 73:1201–1223, 1993
19. Chen JD, McCallum RW: Clinical applications of electrogastrography. Am J Gastroenterol 88:1324–1336, 1993
20. Chen JD, Pan J, McCallum RW: Clinical significance of gastric myoelectrical dysrhythmias. Dig Dis 13:275–290, 1995
21. Huizinga JD, Thuneberg L, Kluppel M, Malysz J, Mikkelsen HB, Bernstein A: *Wlkit* gene required for interstitial cells of Cajal and for intestinal pacemaker activity. Nature 373(6512):347–349, 1995
22. Neumark H, Halevi A, Amir S, Yerushalmi S: Assay and use of magnesium ferrite as a reference in absorption trials with cattle. J Dairy Sci 58:1476–1481, 1975
23. Benmair Y, Dreyfuss F, Fischel B, Frei EH, Gilat T: Study of gastric emptying using a ferromagnetic tracer. Gastroenterology 73:1041–1045, 1977
24. Benmair Y, Fischel B, Frei EH, Gilat T: Evaluation of a magnetic method for the measurement of small intestinal transit time. Am J Gastroenterol 68:470–475, 1977
25. Di Luzio S, Comani S, Romani GL, Basile M, Del Gratta C, Pizzella VA: Biomagnetic method to study gastrointestinal activity. Nuovo Cimeto 11D:1853–1859, 1989
26. Trahms L, Stehr R, Wedemeyer J, Weitschies W: Magnetische Marker im Gastrointestinaltrakt-eine neue Methode zum Stu-

dium der Aufnahme fester oraler Arzneiformen. Biomed Tech Berlin 35:158–159, 1990
27. Macri MA, Basile M, Carriero A, Casciardi S, Comani S, Del Gratta C, Di Donato L, Di Luzio S, Neri M, Pasquarelli A, Pizzella V, Romani GL: Measurement of gastrointestinal transit time by means of biomagnetic instrumentation: preliminary results. Clin Phys Physiol Meas 12:(Suppl. A)111–115, 1991
28. Basile M, Neri M, Carriero A, Casciardi S, Comani S, Del Gratta C, Di Donato L, Di Luzio S, Macri MA, Pasquarelli A, Pizzella V, Romani GL: Measurement of segmental transit through the gut in man. A novel approach by the biomagnetic method. Dig Dis Sci 37:1537–1543, 1992
29. Golzarian J, Staton DJ, Wikswo JP Jr, Friedman RN, Richards WO: Diagnosing intestinal ischemia using a noncontact superconducting quantum interference device. Am J Surg 167:586–592, 1994
30. Richards WO, Garrard CL, Allos SH, Bradshaw LA, Staton DJ, Wikswo JP Jr: Noninvasive diagnosis of mesenteric ischemia using a SQUID magnetometer. Ann Surg 22:696–704, 1995
31. Allos SH, Sorrell M, Slater S, Staton D, Wikswo JP Jr, Richards WO: SQUID magnetometer diagnosis of mesenteric vein Thrombosis. Gastroenterology 108:A269, 1995
32. Garrad CL, Wikswo JP Jr, Staton D, Golzarian J, Gallen C, Richards WO: Noninvasive measurement of small bowel electrical activity. Gastroenterology 106:A502, 1994
33. Abraham-Fuchs K, Schneider S, Reichenberger H: MCG inverse solution: Influence of coil size, number of coils, and SNR. IEEE Trans Biomed Eng 35:573–576, 1988
34. Gudden F, Hoenig E, Reichenberger H, Schittenhelm R, Schneider G: Ein Vielkanalsystem zur Biomagnetischen Diagnostik in Neurologie und Kardiologie: Prinzip, Methode und erste Ergebnisse. Elektromedica 57:2–7, 1989
35. Hoenig HE, Daalmans G, Folberth W, Reichenberger H, Schneider S, Seifert H: Biomagnetic multichannel system with integrated SQUIDs and first order gradiometers operating in a shielded room. Cryogenics 29:809–813, 1989
36. Abraham-Fuchs K, Harer W, Schneider S, Stefan H: Pattern recognition in biomagnetic signals by spatio-temporal correlation and application to the localisation of propagating neuronal activity. Med Biol Eng Comput 28:398–406, 1990
37. Abraham-Fuchs K, Schneider S, Stefan H: Principles of magnetoelencephalography. *In* Focus Localization. Pawlik G, Stefan H. (eds). Symp Köln 1996, pp 247–259
38. Richards WO, Garrard CL, Allos SH, Bradshaw LA, Staton DJ, Wilkswo JP Jr: Noninvasive diagnosis of mesenteric ischemia using a SQUID magnetometer (discussion). Ann Surg 22:704–705, 1995